

Neural Block Sampling

Tongzhou Wang
EECS, UC Berkeley

Yi Wu
EECS, UC Berkeley

David A. Moore
EECS, UC Berkeley

Stuart J. Russell
EECS, UC Berkeley

Abstract

Efficient Monte Carlo inference often requires manual construction of model-specific proposals. We propose an approach to automated proposal construction by training neural networks to provide fast approximations to block Gibbs conditionals. The learned proposals generalize to occurrences of common structural motifs both within a given model and across different models, allowing for the construction of a library of learned inference primitives that can accelerate inference on unseen models with no model-specific training required. We explore several applications including open-universe Gaussian mixture models, in which our learned proposals outperform a hand-tuned sampler, and a real-world named entity recognition task, in which our sampler’s ability to escape local modes yields higher final F1 scores than single-site Gibbs.

1 INTRODUCTION

Model-based probabilistic inference is a highly successful paradigm for machine learning, with applications to tasks as diverse as movie recommendation (Stern et al., 2009), visual scene perception (Kulkarni et al., 2015), music transcription (Berg-Kirkpatrick et al., 2014), and monitoring nuclear tests (Moore and Russell, 2017), among many others. People learn and plan using mental models, and indeed the entire enterprise of modern science can be viewed as constructing a sophisticated hierarchy of models of physical, mental, and social phenomena. *Probabilistic programming* provides a formal representation of models as sample-generating programs, promising the ability to explore a rich range of models.

This requires us to perform efficient inference in novel models, motivating the development of black-box inference techniques.

Unfortunately, generic inference methods such as single-site Gibbs sampling (Spiegelhalter et al., 1996) often perform poorly, suffering from slow mixing and being stuck in local optima. Effective real-world inference often requires block proposals that update multiple variables together to overcome near-deterministic and long-range dependence structures. However, computing exact Gibbs proposals for large blocks quickly becomes intractable (approaching the difficulty of posterior inference), and in practice it is common to invest significant effort in hand-engineering proposals specific to a particular model.

In this work, we propose to learn tractable block samplers, in the form of approximate Gibbs proposals, that can then be reused both within a given model and across models containing similar structural motifs. Recent work has recognized that a wide range of models can be represented as compositions of simple components (Grosse et al., 2012), and that domain-specific models may still reuse general structural motifs such as chains, grids, rings, or trees (Kemp and Tenenbaum, 2008). By learning flexible samplers, we can improve inference not only within a specific model but even on previously unseen models containing similar structures, with no additional training required. In contrast to techniques that compile inference procedures specific to a given model (Stuhlmüller et al., 2013; Le et al., 2017; Song et al., 2017), learning inference artifacts that generalize to novel models is valuable in allowing model builders to quickly explore a wide range of possible models.

We explore the application of our approach to a wide range of models. On grid-structured models from a UAI inference competition, our learned proposal significantly outperforms Gibbs sampling even given no model-specific training. For open-universe Gaussian mixture models, we show that a simple learned block proposal yields performance comparable to a model-specific hand-tuned sampler, and generalizes to models more than those it was trained on. We additionally ap-

ply our method to a named entity recognition (NER) task, showing that not only do our learned block proposals mix effectively, the ability to escape local modes yields higher-quality solutions than the standard Gibbs sampling approach.

2 RELATED WORK

There have been great interests in using learned, feedforward inference networks to generate approximate posteriors. Variational autoencoders (VAE) train an inference network jointly with the parameters of the forward model to maximize a variational lower bound (Kingma and Welling, 2013). Within the VAE framework, Burda et al. (2015) and Gu et al. (2015) utilize another neural network as an adaptive proposal distribution to improve the convergence of variational inference. However, the use of a parametric variational distribution means they typically have limited capacity to represent complex, potentially multimodal posteriors, such as those incorporating discrete variables or structural uncertainty.

A related line of work has developed data-driven proposals for importance samplers (Paige and Wood, 2016; Le et al., 2017; Ritchie et al., 2016), training an inference network from prior samples which is then used as a proposal given observed evidence. In particular, Le et al. (2017) generalize the framework to probabilistic programming, and is able to automatically generate and train a neural proposal network given an arbitrary model described in a probabilistic program. Our approach differs in that we focus on MCMC inference, allowing modular proposals for subsets of model variables that may depend on latent quantities, and exploit recurring substructure, and that generalize to new models containing analogous structures with no additional training.

Several approaches have been proposed for adaptive block sampling, in which sets of variables exhibiting strong correlations are identified dynamically during inference, so that costly joint sampling is used only for blocks where it is likely to be beneficial (Venugopal and Gogate, 2013; Turek et al., 2016). This is largely complementary to our current approach, which assumes the set of blocks (structural motifs) is given and attempts to learn fast approximate proposals.

There are exciting recent works that train model-specific MCMC proposals with machine learning techniques. Using adversarial training, Song et al. (2017) directly optimize the similarity between posterior values and proposed values from a symmetric MCMC proposal parametrized by a special neural network architecture. Considering stochastic inverses of graphical models, Inverse MCMC by Stuhlmüller et al. (2013) learns Gibbs-

like proposals from training density estimators using either prior or posterior data. However, both works have limitations on applicable models and require bootstrapping as well as model-specific training using global information, *e.g.*, samples containing all variables. This work differ in that our approach is simpler and more scalable, requiring only local information and generating local proposals that may be reused both within and across different models. Section 4.1.2 explores this comparison with Inverse MCMC empirically.

Taking a much broader view, the approach in this work of learning an approximate local update scheme can be seen as related to approximate message passing (Ross et al., 2011; Heess et al., 2013), and to recent advances in learning gradient-based optimizers for continuous objectives (Andrychowicz et al., 2016; Li and Malik, 2017).

3 NEURAL BLOCK MCMC

In this work, we propose a framework of using a neural network to approximate the Gibbs proposal for a block of variables. Each learned proposal is specific to a particular block structure and a conditioning set corresponding to an approximate Markov blanket. Together we refer to these components as a *structural motif*. Crucially our proposals do *not* fix the model parameters, which are instead provided as network input, so that the same trained network may be reused to perform inference on novel models with parameterizations not previously observed.

Our inference networks are parameterized as mixture density networks (Bishop, 1994), and trained to minimize the KL divergence between the true posterior conditional and the approximate proposal, given prior samples generated from the model. The approximate proposals are then accepted or rejected following the Metropolis-Hastings (MH) rule (Andrieu et al., 2003), so that we maintain the correct stationary distribution even though the proposals are approximate. The following sections describe our approach in more detail.

3.1 Background

Although our approach generalizes to arbitrary probabilistic programs, for simplicity we focus on models represented as factor graphs. A model consists of a set of variables V represented as the nodes of a graph $G = (V, E)$, along with a set of factors specifying a joint probability distribution $p_\Psi(V)$ described by parameters Ψ . In particular, this paper focuses primarily on directed models, in which the factors Ψ specifies the conditional probability distributions of each variable given its parents. In undirected models, such as the CRFs in Sec. 4.3, the factors are arbitrary functions associated with cliques

in the graph (Koller and Friedman, 2009).

Given observations of a set of evidence variables, inference attempts to compute (by way of drawing samples) the conditional distribution on the remaining variables. A standard approach is Gibbs sampling (Spiegelhalter et al., 1996; Andrieu et al., 2003), in which each variable v_i is successively resampled from its conditional distribution $p(v_i|V_{-i})$ given all other variables V_{-i} in the graph. In most cases this conditional in fact depends only on a subset of V_{-i} , known as the *Markov blanket*, $\text{MB}(v_i) \subseteq V_{-i}$. Each Gibbs update can be viewed as a MH proposal that is accepted by construction, thus inheriting the MH guarantee that the limiting distribution of the sampling process is the desired posterior conditional distribution (Andrieu et al., 2003).

In models with tight coupling between adjacent variables, proposals that only resample a single variable at a time will tend to mix very slowly. In many cases it is necessary to resample multiple variables simultaneously, i.e., a block proposal. Block proposals can yield much faster mixing per step, but each step is much slower; the cost of computing and storing the block conditional distribution is generally exponential in the size of the block, becoming intractable for large blocks. This motivates the approach in this paper, in which we train fast, feedforward neural networks to approximate block proposals at much lower computational cost.

3.2 Structural Motifs in Graphical Models

We associate each learned proposal with a *structural motif* that determines the shape of the network inputs and outputs. In general, structural motifs can be arbitrary subgraphs, but we are more interested in motifs that represent interesting conditional structure between two sets of variables, the block proposed variables B and the conditioning variables C . A given motif can have multiple instantiations with a model, or even across models. As a concrete example, Fig. 1 shows two instantiations of a structural motif of six consecutive variables in a chain model. In each instantiation, we want to approximate the conditional distribution of two middle variables given neighboring four.

We now formalize the notion of a structural motif.

Definition. A structural motif (B, C) (or motif in short) is an (abstract) graph with nodes partitioned into two components, B and C , and a parameterized joint distribution $p(B, C)$ whose factorization is consistent with the graph structure. This specifies the functional form of the conditional $p(B|C)$, but not the specific parameters.

A motif may have many instantiations within a particular graphical model as well as across different models.

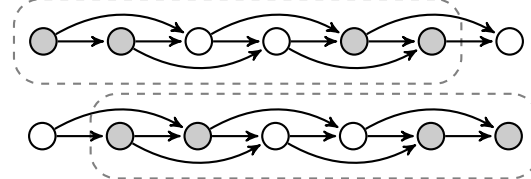


Figure 1: Two instantiations of a structural motif in a directed chain of length 7. The motif consists of two consecutive variables and their Markov blanket of four neighboring variables. Each instantiation is separated into block proposed variables B_i (white) and conditioning variables C_i (shaded).

Definition. For a graphical model $(G = (V, E), \Psi)$, an instantiation (B_i, C_i, Ψ_i) of a motif (B, C) includes

1. a subset of the model variables $(B_i, C_i) \subseteq V$ such that the induced subgraph on (B_i, C_i) is isomorphic to the motif (B, C) with the partition preserved by the isomorphism (so nodes in B are mapped to B_i , and C to C_i), and
2. a subset of model parameters $\Psi_i \subseteq \Psi$ required to specify the joint distribution $p_{\Psi_i}(B, C)$ on motif variables.

We would typically define a structural motif by first picking out a block of variables B to jointly sample, and then selecting a conditioning set C . Intuitively, the natural choice for a conditioning set is the Markov blanket, $C = \text{MB}(B)$. However, this is not a fixed requirement, and C could be either a subset or superset of it (or neither). We might deliberately choose to use some alternate conditioning set C , e.g., a subset of the Markov blanket to gain a faster proposal, or a superset with the idea of learning longer-range structure. More fundamentally, however, Markov blankets depend on the larger graph structure might not be consistent across instantiations of a given motif (e.g., if one instantiation has additional edges connecting B_i to other model variables not in C_i). Allowing C to represent a generic conditioning set leaves us with greater flexibility in instantiating motifs.

Formally, our goal is to learn a Gibbs-like block proposal $q(B_i|C_i; \Psi_i)$ for all instantiations of a structural motif $\{(B_i, C_i, \Psi_i)\}_i$ that is close to the true conditional in the sense that $\forall i, \forall c_i \in \text{supp}(C_i)$,

$$q(B_i; c_i, \Psi_i) \approx p_{\Psi}(B_i|C_i = c_i) \quad (1)$$

This provides another view of this approximation problem. If we choose the motif to have complex structures in each instantiation, the conditionals $p_{\Psi}(B_i|C_i = c_i)$ can often be quite different for different i , and thus difficult to approximate. Therefore, choosing what is a structural motif represents a trade-off between generality of the proposal and easiness to approximate. While our approach works for any structural motif complying with the above definition, we suggest using common structures as motifs, such as chain of certain length as in Fig. 1.

In principle, recurring motifs could be automatically detected, but in this work, we focus on hand-identified commons structures.

3.3 Parameterizing Neural Block Proposals

We choose mixture density networks (MDN) (Bishop, 1994) as our proposal parametrization. An MDN is a form of neural network whose outputs parametrize a mixture distribution, where in each mixture component the variables are uncorrelated. Given a sufficiently large network and number of mixture components, MDNs can represent arbitrary joint distributions.

In our case, a neural block proposal is a function q_θ parametrized by a MDN with weights θ . The function q_θ represents proposals for a structural motif $\{(B_i, C_i, \Psi_i)\}_i$ by taking in current values of C_i and local parameters Ψ_i and outputting a distribution over B_i . Then, the goal becomes to optimize θ so that q_θ is close to the true conditional.

In the network output, mixture weights are represented explicitly. Within each mixture component, distributions of bounded discrete variables are directly represented as probability tables, and distributions of continuous variables are represented as isotropic Gaussians with mean and variance. To avoid degenerate proposals, we threshold the variance of each Gaussian component to be at least 0.00001.

3.4 Training Neural Block Proposals

To optimize our MDN, we use the Kullback-Leibler divergence $D(p_\Psi(B_i|C_i) \parallel q_\theta(B_i; C_i, \Psi_i))$ as the measure of closeness between our proposal and the true conditional in Eq. 1. In order to minimize this divergence across all instantiations (B_i, C_i, Ψ_j) and all possible values in $\text{supp}(C_i)$, our total loss will be a linear combination of expected divergences of all instantiations.

In particular, for an instantiation (B_i, C_i, Ψ_i) , the expected divergence over C_i 's prior is

$$\mathbb{E}_{C_i}[D(p_\Psi(B_i|C_i) \parallel q_\theta(B_i; C_i, \Psi_i))] \quad (2)$$

$$= \mathbb{E}_{C_i}[\mathbb{E}_{B_i|C_i}[\log \frac{p_\Psi(B_i|C_i)}{q_\theta(B_i; C_i, \Psi_i)}]] \quad (3)$$

$$= -\mathbb{E}_{B_i, C_i}[\log q_\theta(B_i; C_i, \Psi_i)] + \text{constant} \quad (4)$$

The second term is a constant independent of θ . Therefore, we define the loss for (B_i, C_i, Ψ_i) as

$$L_i(\theta) = -\mathbb{E}_{B_i, C_i}[\log q_\theta(B_i; C_i, \Psi_i)] \quad (5)$$

In this work, given N instantiations, we define the overall

Algorithm 1 Neural Block MCMC

Input: Graphical model (G, Ψ) , observations y , motifs $\{(B^{(m)}, C^{(m)}, \Psi^{(m)})\}_m$, and instantiations $\{(B_i^{(m)}, C_i^{(m)}, \Psi_i^{(m)})\}_{i,m}$ in (G, Ψ) .

- 1: **for** motif with instantiation $\{(B_i^{(m)}, C_i^{(m)}, \Psi_i^{(m)})\}_i$ **do**
- 2: **if** exists proposal trained for this motif **then**
- 3: $q^{(m)} \leftarrow$ trained neural block proposal
- 4: **else**
- 5: Initialize neural block proposal $q_\theta^{(m)}$
- 6: Train $q_\theta^{(m)}$ using prior samples from (G, Ψ)
- 7: **end if**
- 8: **end for**
- 9: $x \leftarrow$ initialize state
- 10: **for** t in $1 \dots M$ **do**
- 11: Propose $x' \leftarrow q_\theta^{(m)}$ on some $B_i^{(m)}, C_i^{(m)}, \Psi_i^{(m)}$
- 12: Accept or reject according to MH rule
- 13: **end for**

loss as the mean instantiation loss:

$$L(\theta) = \frac{1}{N} \sum_{i=1}^N L_i(\theta) \quad (6)$$

$$= -\frac{1}{N} \sum_{i=1}^N \mathbb{E}_{B_i, C_i}[\log q_\theta(B_i; C_i, \Psi_i)] \quad (7)$$

Since the loss L is an average of expected values over priors, we train our neural block proposals using minibatch SGD. For each training sample in a batch of size K , we randomly select a motif instantiation, and generate sample values from the prior defined for that instantiation. Specifically, for batch index $j \in \{1, \dots, K\}$,

$$i_j \sim \text{Unif}\{1, \dots, N\} \quad (8)$$

$$b_j, c_j \sim p_\Psi(B_{i_j}, C_{i_j}) \quad (9)$$

$$\hat{L}(\theta) = -\frac{1}{K} \sum_{j=1}^K \log q_\theta(b_j; c_j, \Psi_{i_j}) \quad (10)$$

3.5 Neural Block MCMC

Neural Block MCMC procedure is outlined in Algorithm 1. It is worth pointing out that our framework allows a great amount of flexibility. One may be only interested in a good proposal for a specific part of a particular model. Then a neural block proposal can be trained with the underlying motif instantiated only in that part. In other cases, in order to learn a general proposal, say for all grid models, one can work with a grid-shaped motif instantiated in every possible grid model, and extend the training procedure described in Sec. 3.4 by modifying Eq. 8 to match an arbitrary distribution over all instantiations. In experiment Sec. 4.1, we use this approach to train a proposal for all binary-valued grid models. Therefore, it is potentially possible to store a library of neural block proposals trained on common motifs to speed up inference on previously unseen models.

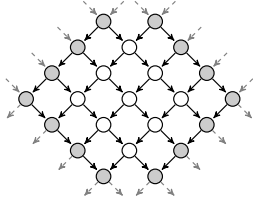


Figure 2: Motif for general grid models. Conditioning variables (shaded) form the Markov blanket of proposed variables (white). Dashed gray arrows show possible but irrelevant dependencies.

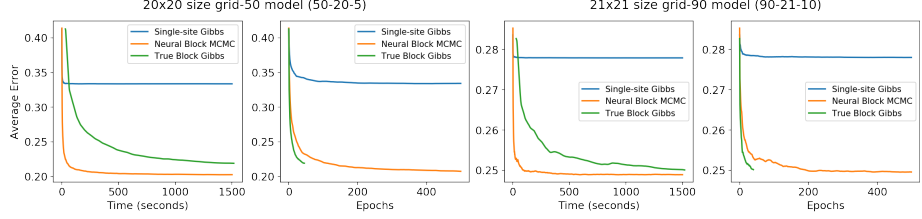


Figure 3: Sample runs with single-site Gibbs, Neural Block MCMC, and block Gibbs with true conditionals. For each model, we compute 10 random initializations and run three algorithms for 1500s on each one. Plots show average error for each algorithm. Epochs plots are cut off at 500 epochs to better show the comparison because true block Gibbs finishes far less epochs than other two within given time.

4 EXPERIMENTS

In this section, we evaluate our method of learning neural block proposals against single-site Gibbs sampler as well as several model-specific MCMC methods. In all experiments, the parameterizing MDNs have elu activation and two hidden layers each of size $\lambda \max \{\text{input size, output size}\}$, where $4 \leq \lambda \leq 5$, and output the proposal distribution as a mixture of $4 \leq m \leq 16$ components. Details on the architecture for each experiment are available in the supplementary material.

4.1 Grid Models

We start with a common structural motif in graphical models, grids. In this section, we focus on binary-valued grid models of all sorts for their relative easiness to directly compute posteriors. Specifically, to test the performance of MCMC algorithms, we compare the estimated posterior marginals \hat{P} against true posterior marginals P computed using IJGP (Mateescu et al., 2010). Then, for each inference task with N variables, we calculated the error $\frac{1}{N} \sum_{i=1}^N |\hat{P}(X_i = 1) - P(X_i = 1)|$ as the mean absolute deviation of marginal probabilities.

4.1.1 General Binary-Valued Grid Models

Neural block proposals have the potential to achieve good performance on models with shared structural motifs without extra training. In our first experiment, we consider the motif in Fig. 2, which is instantiated in arbitrary binary-valued grid Bayesian networks (BN). The neural block proposal takes in CPTs of all $9 + 14 = 23$ variables as well as the current assignments of 14 conditioning variables in Markov blanket.

In order for the proposal to generalize, we need to consider motif instantiations in all possible binary-valued grid models, as argued in Sec. 3.5. We thus train the proposal on random grid BNs generated by sampling each CPT entry i.i.d. from the following mixed distribution:

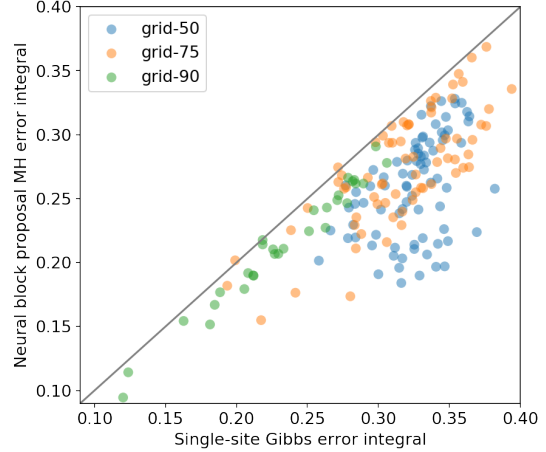


Figure 4: Performance comparison on 180 grid models from UAI 2008 inference competition. Each mark represents error integrals for both single-site Gibbs and our method in a single run over 1200s inference.

$$\begin{cases} [0, 1] & \text{w.p. } \frac{1}{40} \\ [1, 0] & \text{w.p. } \frac{1}{40} \\ \text{Dirichlet}([0.5, 0.5]) & \text{w.p. } \frac{19}{20} \end{cases} \quad (11)$$

After training, the proposal is completely fixed. No model specific optimization is done in inference time.

We evaluate the performance of the trained neural block proposal on all 180 grid BNs up to 500 nodes from UAI 2008¹ inference competition. In each epoch, for each latent variable, we try to identify and propose the block as in Fig. 6 with the variable located at center. If this is not possible, e.g., the variable is at boundaries or close to evidence, single-site Gibbs resampling is used instead.

Figure 4 shows the performance of both Neural Block MCMC and single-site Gibbs in terms of error integrated over time for all 180 models. The models are divided into three classes, grid-50, grid-75 and grid-90, according to the percentage of deterministic relations. Our Neural Block MCMC significantly outperforms Gibbs sampler in nearly every model. We notice that the improvement is less significant as the percentage of deter-

¹<http://graphmod.ics.uci.edu/uai08>

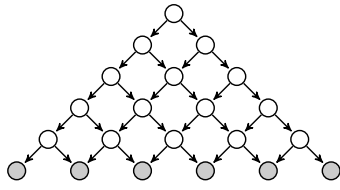


Figure 5: Small version of the triangle grid model in experiment Sec. 4.1.2. Evidence nodes (shaded) are at bottom layer. The actual network has 15 layers and 120 nodes.

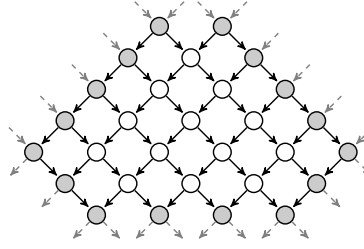


Figure 6: Motif for the triangle model in Fig. 5. Conditioning variables (shaded) form the Markov blanket of proposed variables (white). Dashed gray arrows are possible irrelevant dependencies.

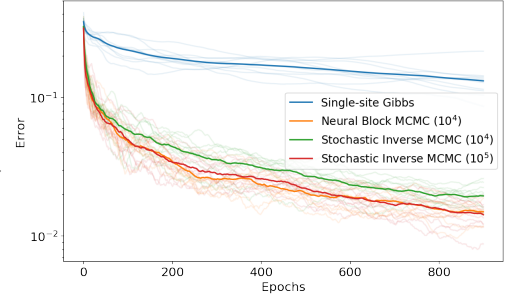


Figure 7: Error w.r.t. epochs on the triangle model in Fig. 5. Semitransparent line show single MCMC runs. Opaque lines show averages over 10 MCMC runs for each algorithm. Numbers in parentheses are the amounts of training data.

ministic relations increases. This is largely due to the fact that the above proposal structure in Fig. 2 can only easily handle dependency among the 9 proposed nodes. We expect an increased block size to yield stronger performance on models with many deterministic relations.

To investigate the behavior of Neural Block MCMC in detail, we compare it against single-site Gibbs, and exact block Gibbs with the same proposal block, on several grid models with different percentages of deterministic relations. Figure 3 shows their performance w.r.t. both time and epochs on two models. Single-site Gibbs performs worst on both models since it gets stuck very quickly in local modes. Between the two block proposal MCMC methods, Neural Block MCMC is more performing in error w.r.t. time due to shorter computational time. However, because the neural block proposal is only an approximate of the true block Gibbs proposal, it is worse in terms of error w.r.t. epochs, as expected. Detailed comparisons on other models are available in supplementary material.

In summary, our experiment results show that neural block proposals can achieve significantly faster and better mixing, while using much less computation overhead than calculating the exact Gibbs block proposal.

4.1.2 Comparison with Inverse MCMC

Neural block proposals can also be used model-specifically by training only on a particular model. In this subsection, we demonstrate that our method can achieve comparable performance with a more complex task-specific MCMC method, Inverse MCMC (Stuhlmüller et al., 2013).

Figure 5 illustrates the triangle grid network we use in this experiment, which is identical to what Stuhlmüller et al. (2013) used to evaluate Inverse MCMC. For our method, we chose the motif shown in Fig. 6. The underlying MDN takes in assignments of conditioning variables and all relevant CPTs, then outputs a block proposal of 13 variables. The proposal is trained on all in-

stantiations in this triangle model using prior samples.

Inverse MCMC is an algorithm that builds auxiliary data structures offline to speed up inference. Given an inference task, it computes and trains an inverse graph for each latent variable where the latent variable is at bottom and evidence variables are at top. These graphs are then used in MCMC procedures. In this experiment, we run Inverse MCMC with frequency density estimator trained with posterior samples, proposal block size up to 20 and Gibbs proposals precomputed, following the original approach of Stuhlmüller et al. (2013).

It is difficult to compare these two methods w.r.t. time. While both methods require offline training, Inverse MCMC needs to train inverse graphs from scratch if the set of evidence nodes changes, yet Neural Block MCMC only needs one-time training for different inference tasks on this model. In this experiment setting, for each inference epoch, both methods propose about 10.5 values on average per latent variable. Figure 7 shows a more meaningful comparison of error w.r.t. epochs among single-site Gibbs, Neural Block MCMC, and Inverse MCMC with different amount of training data. The learned neural block proposal, trained using 10^4 samples, is able to achieve comparable performance with Inverse MCMC, which is trained using 10^5 samples and builds model-specific data structure (inverse graphs).

4.2 Gaussian Mixture Model with Unknown Number of Components

We next consider open-universe Gaussian mixture models (GMMs), in which the number of mixture components is unknown, subject to a prior. Similarly to Dirichlet process GMMs, these are typically treated with hand-designed model-specific split-merge MCMC algorithms.

Specifically, we study the performance of Neural Block MCMC and split-merge Gibbs on a GMM shown in Fig. 9. In this setting, n points $\mathbf{x} = \{x_i\}_{i=1,\dots,n}$ are observed from the GMM with unknown number of active

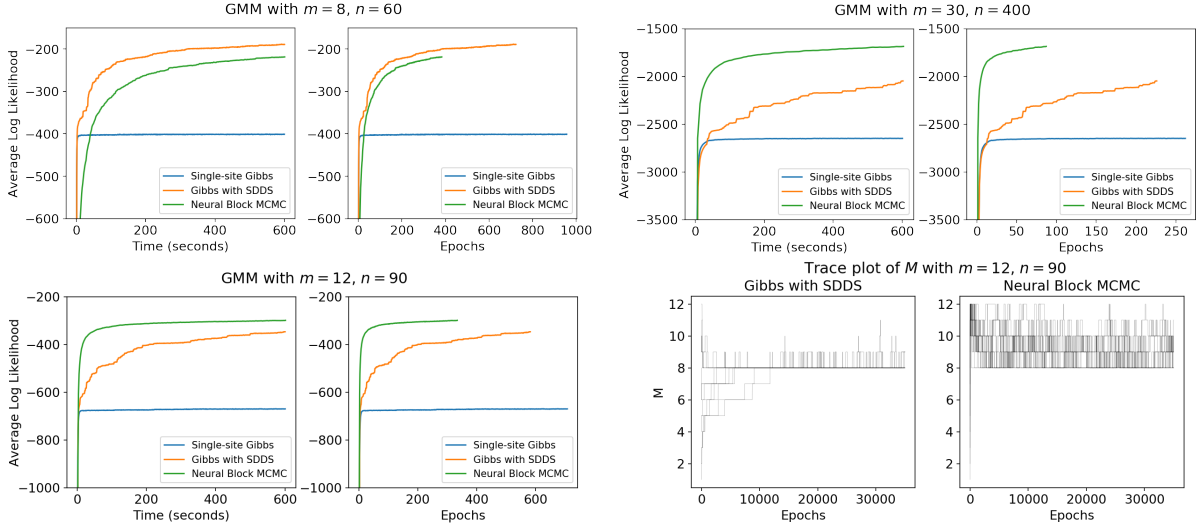


Figure 8: **All except bottom right:** Average log likelihoods of MCMC algorithms run on 200 inference tasks for a total of 600s in various GMMs. **Bottom right:** Trace plots of M over 12 runs from initiations with different M values on a GMM with $m = 12$, $n = 90$. Neural Block MCMC explores the sample space significantly faster than Gibbs with SDDS.

mixtures $M \sim \text{Unif}\{1, 2, \dots, m\}$. Each point comes uniformly randomly from one of the M active mixtures. Our task is to infer the posterior of mixture means $\mu = \{\mu_j\}_{j=1, \dots, M}$, their indicators showing whether active or not $\mathbf{v} = \{v_j\}_{j=1, \dots, M}$, and the labels $\mathbf{z} = \{z_i\}_{i=1, \dots, n}$, where z_i is the mixture index x_i comes from. Formally, the model can be written as:

$$\begin{aligned} M &\sim \text{Unif}\{1, 2, \dots, m\} \\ \mu_j &\sim \mathcal{N}(0, \sigma_\mu^2 I) \quad j = 1, \dots, m \\ \mathbf{v}|M &\sim \text{Unif}\{a \in \{0, 1\}^m : \sum a_j = M\} \\ z_i|\mathbf{v} &\sim \text{Unif}\{j : v_j = 1\} \quad i = 1, \dots, n \\ x_i|z_i, \mu &\sim \mathcal{N}(\mu_{z_i}, \sigma^2 I) \quad i = 1, \dots, n, \end{aligned}$$

where m, n, σ_μ^2 and σ^2 are model parameters. Notice that M is completely dependent of \mathbf{v} , so in this experiment, we always calculate $M = \sum_j v_j$ instead of sampling M .

The GMM's many nearly-deterministic relations, e.g., $p(v_j = 0, z_i = j) = 0$, can cause vanilla single-site Gibbs stuck in local optima and unable to efficiently explore the state space by jumping across different M values. To solve such issues, split-merge MCMC algorithms, such as Restricted Gibbs split-merge (RGSM) (Jain and Neal, 2004) and Smart-Dumb/Dumb-Smart (SDDS) (Wang and Russell, 2015), use hand-designed model-specific MCMC moves that split and merge mixture components.

For Neural Block MCMC framework, it is possible to deal with such nearly-deterministic relations with a proposal block including all of \mathbf{z} , μ and \mathbf{v} . However, doing so would require a long training time of a large network and cause the resulting proposal not able to generalize to GMMs of various sizes.

Instead, we consider the model with \mathbf{z} variables collapsed and train a proposal q_θ for two arbitrary mixtures (μ_i, v_i) and (μ_j, v_j) conditioned on all other variables (excluding \mathbf{z}). The inference task is indeed equivalent to first sampling μ, \mathbf{v} from the collapsed model $p(\mu, \mathbf{v}|\mathbf{x})$ and then sampling \mathbf{z} from $p(\mathbf{z}|\mu, \mathbf{v}, \mathbf{x})$. We modify the algorithm such that the proposal from q_θ is accepted or rejected by the MH rule on the *collapsed* model. Afterwards, \mathbf{z} is resampled from $p(\mathbf{z}|\mu, \mathbf{v}, \mathbf{x})$. This approach is less sensitive to different n values and leads to good performance in variously sized GMMs, as will be shown below. More details on this are in the supplementary material.

In training, we notice that such mixture models have symmetries that must be broken before used as input to the neural network (Nishihara et al., 2013). In particular, the mixtures $\{(v_j, \mu_j)\}_j$ can be permuted in $m!$ ways and the points $\{(z_i, x_i)\}_i$ in $n!$ ways. Following a similar procedure by Le et al. (2017), we sort these values according the first principal component of \mathbf{x} , and also feed the first principal component vector into the MDN. Using prior samples, we are able to train a neural block proposal for the mentioned structural motif. In inference, we randomly choose two clusters to propose at each proposal.

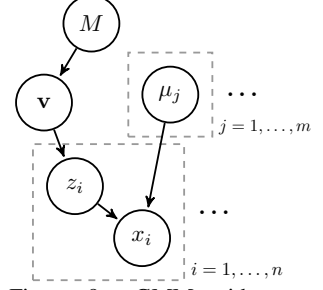


Figure 9: GMM with unknown number of components M , component means μ , and N observed points x_i with cluster labels z_i . We represent the open-universe model in truncated form, where each v_j determines whether the j th cluster is active, so that $\sum_j v_j = M$ deterministically.

Although our proposal is trained on a GMM with a specific number of mixtures $m = 8$ and number of points $n = 60$, we also apply it on GMMs with larger m and n by randomly selecting 8 mixtures and 60 points for each proposal. Figure 8 shows how the Neural Block MCMC performs on GMM of various sizes, compared against split-merge Gibbs with SDDS. In particular, we notice that as model gets larger, Gibbs with SDDS mixes more slowly, while Neural Block MCMC still mixes fairly fast and outperforms Gibbs with SDDS. Bottom right of Fig. 8 shows a trace plot of M for both algorithms over multiple runs on the same observation. Gibbs with SDDS takes a long time to find a high likelihood explanation and fails to explore other possible ones efficiently. Neural Block MCMC, on the other hand, mixes quickly among the possible explanations.

4.3 Named Entity Recognition (NER) Tagging

Named entity recognition (NER) is the task of inferring named entity tags for words in natural language sentences. One way to tackle NER is to train a conditional random field (CRF) model representing the joint distribution of tags and word features (Liang et al., 2008). In particular, the model contains weights between word features and tags as well as high order factors of consecutive tags. For each test sentence, we can build a chain Markov random field (MRF) containing only the tags variables using extracted word features and learned CRF model, and then apply MCMC methods like single-site Gibbs to sample the NER tags. For this experiment, we use a dataset of 17494 sentences taken from CoNLL-2003 Shared Task². The CRF model is trained with AdaGrad (Duchi et al., 2011) through 10 sweeps over the training dataset.

Our goal is to train good neural block proposals for the chain MRFs built for test sentences. In order to experiment with different block sizes, we train three proposals, each for a motif of two, three, or four consecutive proposed tag variables and their Markov blanket. With each proposal, the MDN takes in both the local MRF parameters and assignments of Markov blanket variables, then outputs the proposal as a mixture of 4 components. Due to the difficulty in generating natural language sentences, we reuse the training dataset for CRF model to train neural block proposals.

We then evaluate the learned neural block proposals on the previously unseen test dataset of 3453 sentences. Figure 10 plots the performance of Neural Block MCMC and single-site Gibbs w.r.t. both time and epochs on the entire test dataset. As block size grows larger, learned proposal takes more time to mix. But even

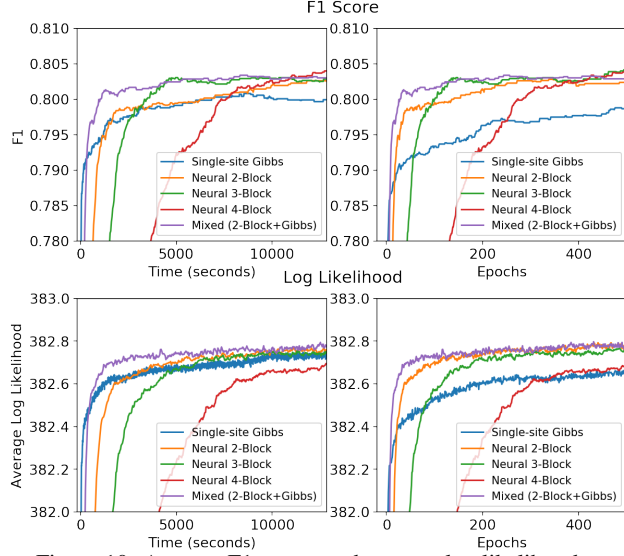


Figure 10: Average F1 scores and average log likelihoods over entire test dataset. In each epoch, all variables in every test MRF is proposed roughly once for all algorithms. F1 scores are measured using states with highest likelihood seen over Markov chain traces. To better show comparison, epoch plots are cut off at 500 epochs and time plots at 12850s. Log likelihoods shown don't include normalization constant.

tually, block proposals generally achieve better performance than single-site Gibbs in terms of both F1 scores and log likelihoods. Therefore, as shown in the figure, a mixed proposal of single-site Gibbs and neural block proposals can achieve better mixing without slowing down much. As an interesting observation, Neural Block MCMC sometimes achieves higher F1 scores even before passing single-site Gibbs in log likelihood, implying that log likelihood is at best an imperfect proxy for performance on this task.

5 CONCLUSION

This paper proposes and explores the (to our knowledge) novel idea of training neural nets to approximate block Gibbs proposals. Our proposals are trained offline and can be applied directly to novel models given only a common set of structural motifs. Experiments show that the neural block sampling approach can help overcome bad local modes comparing with single-site Gibbs sampling and achieve comparable performance against model-specialized methods.

In the current stage, our framework requires the user to manually detect common structural motifs and choose where and how to apply the pretrained block sampler. It will be a very interesting direction to investigate, when given a library of trained block proposals, how an inference system can automatically detect the common structural motifs and (adaptively) apply appropriate samplers to help convergence for real-world applications.

²<http://www.cnts.ua.ac.be/conll2003/ner/>

References

Christophe Andrieu, Nando De Freitas, Arnaud Doucet, and Michael I Jordan. An introduction to MCMC for machine learning. *Machine learning*, 50(1):5–43, 2003.

Marcin Andrychowicz, Misha Denil, Sergio Gómez, Matthew W Hoffman, David Pfau, Tom Schaul, and Nando de Freitas. Learning to learn by gradient descent by gradient descent. In D. D. Lee, M. Sugiyama, U. V. Luxburg, I. Guyon, and R. Garnett, editors, *Advances in Neural Information Processing Systems 29*, pages 3981–3989. Curran Associates, Inc., 2016.

Taylor Berg-Kirkpatrick, Jacob Andreas, and Dan Klein. Unsupervised transcription of piano music. In *Advances in neural information processing systems*, pages 1538–1546, 2014.

Christopher M Bishop. Mixture density networks. 1994.

Yuri Burda, Roger Grosse, and Ruslan Salakhutdinov. Importance weighted autoencoders. *arXiv preprint arXiv:1509.00519*, 2015.

John Duchi, Elad Hazan, and Yoram Singer. Adaptive subgradient methods for online learning and stochastic optimization. *Journal of Machine Learning Research*, 12(Jul):2121–2159, 2011.

Roger Grosse, Ruslan R Salakhutdinov, William T Freeman, and Joshua B Tenenbaum. Exploiting compositionality to explore a large space of model structures. In *28th Conference on Uncertainty in Artificial Intelligence*, pages 15–17. AUAI Press, 2012.

Shixiang Gu, Zoubin Ghahramani, and Richard E Turner. Neural adaptive sequential Monte Carlo. In *Advances in Neural Information Processing Systems*, pages 2629–2637, 2015.

Nicolas Heess, Daniel Tarlow, and John Winn. Learning to pass expectation propagation messages. In *Advances in Neural Information Processing Systems*, pages 3219–3227, 2013.

Sonia Jain and Radford M Neal. A split-merge Markov chain Monte Carlo procedure for the Dirichlet process mixture model. *Journal of Computational and Graphical Statistics*, 13(1):158–182, 2004.

Charles Kemp and Joshua B Tenenbaum. The discovery of structural form. *Proceedings of the National Academy of Sciences*, 105(31):10687–10692, 2008.

Diederik P Kingma and Max Welling. Auto-encoding variational Bayes. *arXiv preprint arXiv:1312.6114*, 2013.

Daphne Koller and Nir Friedman. *Probabilistic graphical models: principles and techniques*. MIT press, 2009.

Tejas D Kulkarni, Pushmeet Kohli, Joshua B Tenenbaum, and Vikash Mansinghka. Picture: A probabilistic programming language for scene perception. In *Proceedings of the ieee conference on computer vision and pattern recognition*, pages 4390–4399, 2015.

Tuan Anh Le, Atlm Gne Baydin, and Frank Wood. Inference Compilation and Universal Probabilistic Programming. In *20th International Conference on Artificial Intelligence and Statistics*, Fort Lauderdale, FL, USA, 2017.

Ke Li and Jitendra Malik. Learning to optimize neural nets. *arXiv preprint arXiv:1703.00441*, 2017.

Percy Liang, Hal Daumé III, and Dan Klein. Structure compilation: trading structure for features. In *Proceedings of the 25th international conference on Machine learning*, pages 592–599. ACM, 2008.

Robert Mateescu, Karel Kask, Vibhav Gogate, and Rina Dechter. Join-graph propagation algorithms. *Journal of Artificial Intelligence Research*, 37(1):279–328, 2010.

David A. Moore and Stuart J. Russell. Signal-based Bayesian seismic monitoring. *Artificial Intelligence and Statistics (AISTATS)*, April 2017.

Robert Nishihara, Thomas Minka, and Daniel Tarlow. Detecting parameter symmetries in probabilistic models. *arXiv preprint arXiv:1312.5386*, 2013.

B. Paige and F. Wood. Inference networks for sequential Monte Carlo in graphical models. In *Proceedings of the 33rd International Conference on Machine Learning*, volume 48 of *JMLR*, 2016.

Daniel Ritchie, Anna Thomas, Pat Hanrahan, and Noah Goodman. Neurally-guided procedural models: Amortized inference for procedural graphics programs using neural networks. In D. D. Lee, M. Sugiyama, U. V. Luxburg, I. Guyon, and R. Garnett, editors, *Advances in Neural Information Processing Systems 29*, pages 622–630. Curran Associates, Inc., 2016.

Stephane Ross, Daniel Munoz, Martial Hebert, and J Andrew Bagnell. Learning message-passing inference machines for structured prediction. In *Computer Vision and Pattern Recognition (CVPR), 2011 IEEE Conference on*, pages 2737–2744. IEEE, 2011.

Jiaming Song, Shengjia Zhao, and Stefano Ermon. A-NICE-MC: Adversarial training for MCMC. *arXiv preprint arXiv:1706.07561*, 2017.

David J Spiegelhalter, Andrew Thomas, Nicky G Best, Wally Gilks, and D Lunn. BUGS: Bayesian inference using Gibbs sampling. *Version 0.5,(version ii) http://www. mrc-bsu. cam. ac. uk/bugs*, 19, 1996.

David H Stern, Ralf Herbrich, and Thore Graepel. Matchbox: large scale online Bayesian recommendations. In *Proceedings of the 18th international conference on World wide web*, pages 111–120. ACM, 2009.

Andreas Stuhlmüller, Jacob Taylor, and Noah Goodman. Learning stochastic inverses. In *Neural Information Processing Systems*, 2013.

Daniel Turek, Perry de Valpine, Christopher J Paciorek, Clifford Anderson-Bergman, et al. Automated parameter blocking for efficient Markov chain Monte Carlo sampling. *Bayesian Analysis*, 2016.

Deepak Venugopal and Vibhav Gogate. Dynamic blocking and collapsing for Gibbs sampling. In *Uncertainty in Artificial Intelligence*, page 664. Citeseer, 2013.

Wei Wang and Stuart J Russell. A smart-dumb/dumb-smart algorithm for efficient split-merge MCMC. In *UAI*, pages 902–911, 2015.

Supplementary Materials: Neural Block Sampling

6 EXPERIMENT DETAILS

As mentioned in main paper Sec. 4, parameterizing MDNs in all experiments have elu activation and two hidden layers each of size $\lambda \max \{\text{input size, output size}\}$, where $4 \leq \lambda \leq 5$ depending on the task, and output the proposal distribution as a mixture of $4 \leq m \leq 16$ components.

6.1 Grid Models

For directed binary-valued grid models, we use higher amount of MDN mixtures than other experiments because more variables are proposed and general discrete BNs can have highly multi-modal conditionals.

6.1.1 General Binary-Valued Grid Models

Architecture The underlying MDN has 106-480-480-120 network structure, mapping the CPTs of all 23 motif variables and 14 conditioning variable values to the proposal distribution of 9 proposed variables as a mixture of 12 components.

Additional Sample Runs We provide additional sample runs on four grid models with various percentages of deterministic relations in Fig. 1.

6.1.2 Comparison with Inverse MCMC

Architecture The underlying MDN has 161-1120-1120-224 network structure, mapping the CPTs of all 29 motif variables and 16 conditioning variable values to the proposal distribution of 13 proposed variables as a mixture of 16 components.

6.2 Gaussian Mixture Model with Unknown Number of Components

Architecture Our neural block proposal is trained using the GMM with $m = 8$ max mixtures and $n = 60$ data points. It proposes two mixture components (μ_j, v_j) s through underlying MDN of 156-624-624-36 network structure. The MDN's inputs include 60 observed points $\mathbf{x} = \{x_i\}_i$, 8 component means $\boldsymbol{\mu} = \{\mu_j\}_j$ and component active indicators $\mathbf{v} = \{v_j\}_j$ with values for the two proposed mixtures replaced by zeros. Orders for

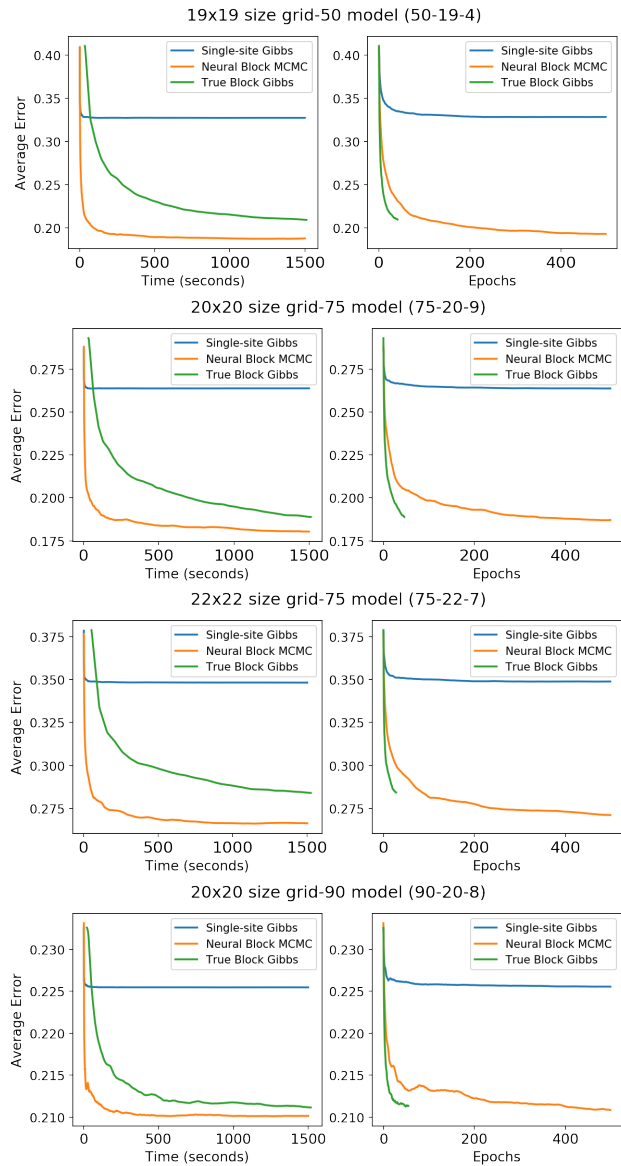


Figure 1: Additional sample runs with single-site Gibbs, neural block MCMC, and block Gibbs with true conditionals on UAI 2008 grid models. These results are obtained in same setting as Fig. 3 of main paper. For each model, we compute 10 random initializations and run three algorithms for 1500s on each one. Plots show average error for each algorithm. Epochs plots are cut off at 500 epochs to better show the comparison. “grid- k ” represents that the model has $k\%$ deterministic relations.

\mathbf{x} , $\boldsymbol{\mu}$ and \mathbf{v} are such that they are sorted along the first principle component of \mathbf{x} to break symmetry. In addition, the inputs also contain the principle component and the indicators of which components are being proposed. The MDN outputs a proposal distribution over the two (μ_j, v_j) s as a mixture of 4 MDN components.

Proposal and Inference with \mathbf{z} Collapsed In order to avoid nearly-deterministic relations, *e.g.*, $p(v_j = 0, z_i = j) = 0$, and still train a general proposal unconstrained by n , we choose to consider the collapsed model without \mathbf{z} . We first experiment on the intuitive approach which adds a resampling step for \mathbf{z} in the proposal. At each proposal step, trained proposal q_θ is first used to propose new mixtures $\boldsymbol{\mu}'$ and \mathbf{v}' , and then \mathbf{z} is proposed from $p(\mathbf{z}|\boldsymbol{\mu}', \mathbf{v}', \mathbf{x})$. The MH rule is applied lastly to either accept or reject all proposed values. While this method gives good performance in small models, it suffers greatly from low acceptance ratio as n , the number of observed points \mathbf{z} , grows large. Therefore, we eventually choose the approach described in main paper Sec. 4.2, *i.e.*, applying the MH rule on the *collapsed* model with \mathbf{z} resampled from $p(\mathbf{z}|\boldsymbol{\mu}, \mathbf{v}, \mathbf{x})$ afterwards. Since the acceptance ratio no longer depends on n , this approach behaves much more scalable than the first one in our experiments. It outperforms SDDS split-merge MCMC in GMMs of various sizes, as shown in Fig. 8 of main paper.

6.3 NER Tagging

Architecture The underlying MDN two hidden layers of size $4 \times \max \{\text{input size, output size}\}$, with output size varying according to the number of proposed variables. It maps local CRF parameters of all motif variables and conditioning variable values to the NER tag proposal for consecutive proposed variables as a mixture of 4 components.